Chemical Engineering Journal 157 (2010) 539–550

Contents lists available at ScienceDirect

Chemical Engineering Journal

journal homepage: www.elsevier.com/locate/cej

Kinetics and modeling of fatty acids esterification on acid exchange resins

R. Tesser, L. Casale, D. Verde, M. Di Serio, E. Santacesaria*

Dipartimento di Chimica, Università degli Studi di Napoli Federico II, Via Cinthia, Complesso Universitario di Monte di Sant'Angelo, 80126 Napoli, Italy

ARTICLE INFO

Article history:
Received 9 November 2009
Received in revised form
22 December 2009
Accepted 24 December 2009

Keywords:
Biodiesel production
FFAs esterification
Ion-exchange resins

ABSTRACT

Biodiesel, a renewable fuel of vegetal origin, has been an object of a rapidly growing interest, in the latest years, both as a pure fuel and as blending component to reduce exhaust pollutants of traditional diesel fuel. Biodiesel is conventionally produced through a well-established technology that involves the use of alkaline catalysts and is, therefore, not compatible with the presence of free fatty acids (FFAs) in the feedstock due to the formation of soaps. Also the presence of FFA in small amounts is detrimental, because, formed soaps strongly affect the successive glycerol separation giving place to a long settling time. Normally, highly refined vegetable oils are used as raw materials for biodiesel production. A preliminary stage of acidity reduction is necessary, when the starting material is characterized by a high free acidity (higher than 0.5% by weight). This pre-treatment can be pursued, as example, by means of an esterification reaction of the FFAs with methanol, catalyzed by sulphonic ionic exchange resins. In the present work, a batch reactor has been used for the study of the above-mentioned reaction and different acid ionic exchange resins have been tested as heterogeneous catalysts. Two kinds of substrates have been submitted for esterification with methanol: a model mixture of soybean oil artificially acidified with oleic acid and a commercial high-acidity mixture of waste fatty acids (oleins). A detailed kinetic model has been developed and tested in which the following key phenomena, characterizing the system, have been introduced: (i) the physical phase equilibrium (partitioning equilibrium) of the components between the resin-absorbed phase and the external liquid phase; (ii) the ionic exchange equilibria; (iii) an Eley–Rideal surface reaction mechanism. The developed kinetic model was able to correctly interpret all the experimental data collected, both as a function of the temperature and of the catalyst concentration.

1. Introduction

Biodiesel represents a valuable alternative to petroleum-derived fuels due to both its renewable nature and its substantially reduced net carbon dioxide emission. This biofuel is conventionally produced through batch or continuous transesterification of highly refined vegetable oils with methanol by using homogeneous alkaline catalysts such as sodium or potassium hydroxides or methoxides [1,2]. The mentioned technology is not compatible with oils which free fatty acids (FFAs) content exceeding a threshold value of about 0.5% by weight. The main limitation for a wider biodiesel market share is represented by the relatively high cost of the raw material: the steps of production, transportation, storage and refining of vegetable oils affect for more than 85% of the total cost of biodiesel [3].

A possible solution to this drawback could be the development of new technologies enabling to employ waste raw materials such as fried oils or mixture of oils from various sources that cannot be treated in the conventional process for their high content in free fatty acids. This perspective discloses the way toward the development of innovative biodiesel production processes such as those based on supercritical methanol [4], or the two-stage process (esterification and transesterification reaction) [5,6]. The esterification reaction of acid oils or fats can then be used both as biodiesel direct production (in the case of substrates with very high content of FFAs) and as pre-treatment step in the framework of a conventional transesterification process (for feedstock with moderate free acidity). The generic esterification reaction of a carboxylic acid with methanol, producing methylester and water, is schematically shown below:

$$\underset{(A)}{RCOOH} + \underset{(M)}{CH_3OH} \rightleftarrows \underset{(E)}{RCOOCH_3} + \underset{(W)}{H_2O}$$

The esterification processes for FFAs abatement are generally promoted by homogeneous acid catalyzed reaction [5,6] or by ionic exchange acid resins as heterogeneous catalysts. These resins are constituted by a cross-linked polymeric matrix on which the active sites for the esterification reaction are represented by protons bonded to sulphonic groups. However, due to their particular structure, these resins are subjected to a remarkable swelling phenomenon [7] when contacted with polar solvents and, considering

* Corresponding author. Tel.: +39 081 674027; fax: +39 081 674026.
E-mail address: elio.santacesaria@unina.it (E. Santacesaria).

1385-8947/$ – see front matter © 2010 Elsevier B.V. All rights reserved.
doi:10.1016/j.cej.2009.12.050

the components involved in the FFAs esterification reaction, the resin shows a high tendency to incorporate mostly both the water formed by reaction and methanol used as esterification agent. This occurs for both the relatively high polarity of water and methanol and for their reduced molecular size that correspond to an increased diffusional rate inside the pores of the polymeric matrix. According to this selective mechanism, in the interior of the resin an environment is created that strongly differs in concentration from the bulk phase. This aspect plays a fundamental role both on kinetics and on chemical equilibrium, because, the reaction occurring almost completely on the internal volume of the resin, is strongly affected by the partitioning of the component between the absorbed and bulk liquid phases. The correct description of the kinetics for such systems requires then additional information (separately collected) regarding the phase partitioning of the various components between the liquid and the absorbed phase. A further complication is represented by the lack of partitioning data collected in correspondence to the reaction temperature. The mentioned phenomenon is widely described in the literature by means of more or less complex models but this aspect is neglected in some papers that deal with the esterification of fatty acids and the experimental data are often correlated by using a pseudo-homogeneous model, mathematically much simpler but inadequate to the interpretation of the real reaction mechanism. An example of this kind of approach is reported by Pasias et al. [8] who have investigated the FFAs esterification reaction catalyzed by Purolite resin and have interpreted their kinetic data by using a pseudo-homogeneous equilibrium model.

Marchetti et al. [9] have studied this reaction by using, on the contrary, basic resins as catalysts like Dowex monosphere 550 A and Dowex upcore Mono A-625 obtaining interesting results, but without introducing a modeling approach. Tesser et al. [10] reported the esterification reaction kinetics of oleic acid with methanol in the presence of triglycerides, catalyzed by acid resin Resindion Relite CFS in a batch reactor. Furthermore, Santacesaria et al. [11,12] have shown that the esterification reaction, performed in a continuous packed bed tubular reactor (PBR), was strongly affected by external mass transfer limitations, while, good results can be achieved by adopting alternative reactor configurations represented by the well stirred slurry reactor (WSSR) and the spray tower loop reactor (STLR).

Many authors have studied the esterification reactions on different cationic exchange resins but mainly related to short chain fatty acids with different alcohols and adopting different kinetic modeling approaches focused on the experimental data correlation but always neglecting the partitioning phenomenon occurring between the interior and the exterior liquid phase with respect to the resins.

For example, Sanz et al. [13] have studied the kinetics of lactic acid esterification reaction with methanol, catalyzed by different acidic resins. These authors have interpreted their results by means of an Eley–Rideal (ER) and a Langmuir–Hinshelwood (LH) model.

Ali and Merchant [14] have reported kinetic results related to the esterification between acetic acid and 2-propanol on different resins interpreting the obtained data with various models: pseudo-homogeneous (PH), Eley–Rideal (ER), Langmuir–Hinshelwood (LH) and a modified Langmuir–Hinshelwood (MLH). The last one contains an empirical exponent, for water concentration, in order to take into account for the greater affinity of water for the catalytic resin. Ali and Merchant [14] have statistically compared the various models tested and the MLH model resulted the best for the description of their experimental data, as a demonstration that the partitioning phenomenon plays a fundamental role in the kinetics description.

Also Yalcinyuva et al. [15] have demonstrated that the phase partitioning and the swelling phenomena cannot be neglected for an accurate description of an esterification process involving ionic exchange resins. In fact, they have investigated the esterification reaction of myristic acid with isopropyl alcohol catalyzed by Amberlyst 15 and they have shown that the water concentration in the reactive mixture resulted always lower than the theoretical value calculated on the basis of the measured acid conversion.

Mazzotti et al. [16] reported a kinetic study of acetic acid esterification with methanol, in the presence of Amberlyst 15 as catalyst in which the partitioning phenomenon has been interpreted on the basis of a Flory–Huggins model.

Popken et al. [17] and Song et al. [18] have studied the reaction of acetic acid with methanol also using Amberlyst 15 as catalyst. A mass-based Langmuir model has been used for describing the absorption, while, the kinetic behavior has been interpreted with LH model. At last, a recent review on properties and uses of exchange resins has been published by Alexandratos [19].

The purpose of our work is, therefore, the study of the esterification reaction performed on the following acid substrates: (i) a model mixture of soybean oil containing controlled amounts of oleic acids; (ii) commercial mixtures of oils and FFA (oleins) characterized by high FFA concentrations (also greater than >95% by wt as oleic acid). Methanol has been chosen as esterification agent, while, selected acid ion-exchange resins are: Amberlyst 15 and Relite CS. The catalyst selection has been based on both a previous catalysts screening activity and on the availability of literature information. As a matter of fact, Amberlyst 15 is one of the more widely used and studied resin and some absorption and kinetic data are available in the literature. Relite CFS has been chosen because it is less expensive.

The experimental runs, performed in a batch reactor, have been interpreted with a new kinetic model based on an ionic exchange reaction mechanism that takes into account also for the physical partitioning effects of the various components of the reacting mixture between the liquid phase internal and external to the resin. This phase partitioning effect has been studied separately by means of some specific measurements, conducted both at 25 and 100 °C for what concerns the binary system methanol–water. A simple partition–absorption model, suitable to be embedded into the kinetic model, has been developed for the description of the experimental binary phase equilibrium data. The absorption model resulted formally equivalent to a Langmuir model based on the resin void volume available for the absorption.

2. Experimental

2.1. Reactants and methods

The used reactants and the related purities are the following: methanol (Aldrich, purity >99%, w/w), oleic acid (Carlo Erba, purity >90%, w/w), and a commercially available acidity-free soybean oil (acidity <0.3%, w/w). The oleins have been furnished by a local company (Parodi S.r.L.) and their acid composition is shown in Table 1.

The resins Amberlyst 15 and Amberlyst 16 have been purchased by Acros Organics, Amberlyst 131 by Sigma–Aldrich and Relite CFS has been purchased by Resindion.

These resins are macroreticular copolymer styrene-DVB in wet form and their characteristics are shown in Table 2. Before the experimental runs, resins have been dried, at 100 °C, for 24 h in a ventilated oven.

The acidity of the resins has been evaluated by titration. A weighed amount of the dry resin has been put in contact with a solution 0.2 M of NaOH in excess. The excess has then been titrated with HCl 0.1 M. For each determination, three different titrations have been made and for the values reported in Table 1 an error of about 3% has been estimated. The bulk densities of

Table 1
Fatty acids weight percent composition of the oleins (determined by GLC analysis).

Caprylic acid, C8	0.16
Caprinic acid, C10	0.2
Lauric acid, C12	2.51
Myristic acid, C14	1.43
Palmitic acid, C16	31.3
Heptadecanoic acid, C17	0.1
Stearic acid, C18	3.49
Oleic acid, C18:1	43.46
Linoleic acid, C18:2	15.40
Linolenic acid, C18:3	1.22
Arachic acid, C20	0.29
Gadolenic acid, C20:1	0.20
Eicosadienoic acid, C20:2	0.05
Behenic acid, C22	0.08
Erucic acid, C22:1	0.06
Tricosanoic acid, C23	0.02
Average molecular weight	272.5 g/mol

the dry and wet resins have been measured in a graduated cylinder of 10 cm^3. Five tests have been made for each determination with an estimated average error of 2% on the values reported in Table 2.

The analysis of the water present into the liquid phase, in partition experiments, was accomplished via GC (HP9850 A gas chromatograph) equipped with a thermoconductivity detector (TCD). The column used for the analysis was a Restek Rt-Q Plot 30 m × 0.32 mm and propan-2-ol was used as external standard. The temperature was programmed to 40 °C for 5 min, then increasing at 10 °C/min to 200 °C. A simple mass balance was made to evaluate the weight percent of water and methanol absorbed by resin. The experimental error associated with this analytical method is below 1%. The device used for partitioning experiments at 100 °C under pressure was the same as for the esterification reaction and is described in details below. Some experimental partitioning data, collected at 100 °C, are reported in Table 3 for, respectively, Amberlyst 15 and Relite CFS resins.

For what concerns the esterification reaction, the withdrawn samples were analyzed by a standard acid–base titration procedure for the evaluation of the free residual acidity. The analysis repeatability has been improved by removing methanol in excess and water formed, in an oven heated at 120 °C under stirring for 20 min, prior to submitting the samples to titration.

A weighed amount of the sample was then dissolved in ethanol, some droplets of phenolphthalein as indicator were added, and the titration is then performed by means of an alkaline 0.1 M KOH solution. The volume of alkaline solution consumed is recorded, and the acidity of the sample can be calculated by means of the following relation:

$$a = \frac{V_{titr} C_{titr} M_{OA}}{1000 m_{sample}} \times 100 \ (\%wt) \quad (1)$$

The acidity evaluated by Eq. (1) is referred to the oil phase (triglyceride + oleic acid + ester) with an error less than 1–2% on the free acidity expressed as weight percent of oleic acid.

The scheme of the experimental apparatus used for both batch esterification runs and phase partitioning experiments under pressure (runs performed at 100 °C) is reported in Fig. 1. The device is composed by a stainless steel tank reactor (volume 0.6 L) equipped with a magnetically driven stirrer and with pressure and liquid phase temperature indicators. The reactor temperature is maintained at the prefixed value, within ±1 °C, by means of an electrical heating device connected to a PID controller. The reactor body is connected to a stainless steel pressurized chamber with a volume of 150 mL by means of which methanol can be added to the reaction system. The system is initially charged with the desired amount of acid oil and catalyst and, when the temperature reached the desired value, methanol is added using a nitrogen overpressure. This instant represents the initial time for the reaction. During the run, small samples of liquid phase were withdrawn by using a line equipped with a stopping valve. In this way the evolution with time of the mixture acidity can be monitored for different reaction times. At the end of the sampling line, immersed in the reaction mixture, a very narrow mesh screen was fitted in order to prevent dragging of catalytic particles in the withdrawn sample that could produce interference with the analysis.

Table 3
Experimental data of phase partition experiments at 100 °C.

Resin	m^R (g)[a]	m^0_W (g)[b]	m^0_M (g)[c]	$w^{0\,d}_W$	$w^{B\,e}_W$
Relite CFS	9.83	1.9	163.73	0.011	0.010
	9.83	4.8	163.73	0.028	0.024
	9.83	5.7	163.73	0.034	0.027
	9.83	7.9	163.73	0.046	0.039
	9.83	12.4	163.73	0.070	0.063
	9.83	16.6	163.73	0.092	0.083
	9.83	17.8	163.73	0.098	0.084
	9.83	19.2	163.73	0.105	0.090
Amberlyst 15	10.00	2.00	157.80	0.013	0.012
	10.00	4.00	157.80	0.025	0.023
	10.00	6.00	157.80	0.037	0.033
	10.00	8.00	157.80	0.048	0.043
	10.00	10.00	157.80	0.060	0.054
	10.00	12.00	157.80	0.071	0.067

[a] Weight of dry resin.
[b] Amount of water.
[c] Amount of methanol.
[d] Weight fraction of water in bulk before adsorption.
[e] Weight fraction of water in bulk after adsorption.

Table 2
Physico-chemical properties of the resins.

Properties	Amberlyst 15	Amberlyst 16	Amberlyst 131	Relite CFS
Matrix[a]	Macroreticular copolymer styrene-DVB	Macroreticular copolymer styrene-DVB	Macroreticular copolymer styrene-DVB	Porous copolymer styrene-DVB
Functional groups[a]	Sulphonics	Sulphonics	Sulphonics	Sulphonics
Cross-linking degree[a]	20–25%	20–25%	20–25%	20–25%
Acidity[b]	4.7 mequiv./g	4.8 mequiv./g	4.8 mequiv./g	5.2 mequiv./g
Particle size range[a]	0.60–0.85 mm	0.60–0.80 mm	0.70–0.80 mm	0.30–1.18 mm
Particle average diameter[a]	0.7 mm	0.7 mm	0.7 mm	0.7 mm
Total exchange capacity[b]	1.6 equiv./L	1.7 equiv./L	1.8 equiv./L	1.7 equiv./L
Maximum operating temperature[a]	120 °C	120 °C	130 °C	140 °C
Bulk density of dry resin[b]	0.553 g/cm^3	–	–	0.588 g/cm^3
Bulk density of dry resin[b]	0.346 g/cm^3	–	–	0.325 g/cm^3

[a] Value from technical datasheet.
[b] Value determined experimentally in the present work.

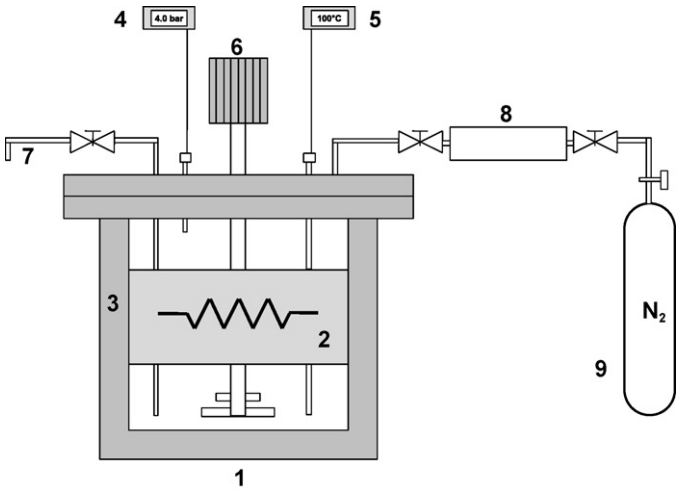

Fig. 1. Batch reactor experimental apparatus. 1: reactor; 2: heating device; 3: rock wool thermal insulation; 4: pressure transducer and indicator; 5: liquid phase thermocouple; 6: magnetically driven stirring device; 7: sampling line; 8: stainless steel pressure chamber for methanol addition; 9: nitrogen cylinder.

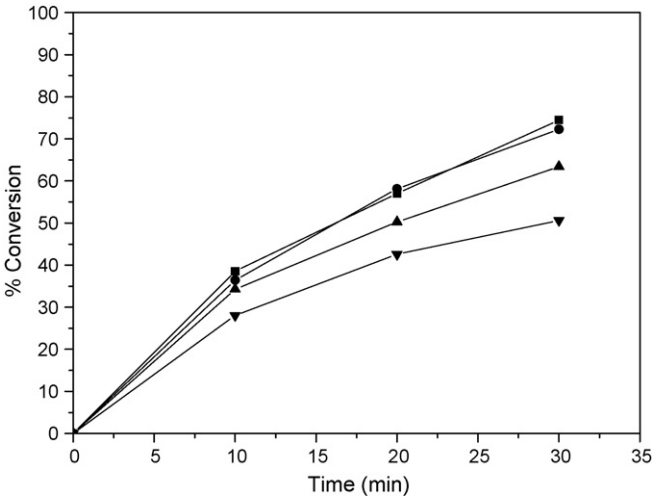

Fig. 2. Experimental batch run at different rpm. Operative conditions: 200 g of oleic acid/soybean oil at 50% of acidity; methanol:oleic acid molar ratio = 8:1; Amberlyst 15 = 5 g; temperature = 120 °C. (▼) 500 rpm, (▲) 1000 rpm, (●) 1200 rpm and (■) 1500 rpm.

In Table 4 are summarized the experimental conditions adopted in each run.

3. Results and discussion

3.1. External diffusive phenomena

A preliminary investigation has been conducted in order to evaluate the influence of mass transfer limitations on the measured kinetic. The extent of the external diffusion has been verified by doing experiments at different stirring rates (500, 1000, 1200 and 1500 rpm), and a constant reaction rate has been observed above the threshold value of about 1200 rpm (see Fig. 2). All the experimental runs have been performed in conditions in which all external diffusive phenomena can be neglected (1500 rpm) and the reactive system can be considered in kinetic regime. The temperature for these specific runs has been fixed at 120 °C, the maximum of the temperature range explored, and with 5 g of Amberlyst 15 as catalyst. For the experimental batch runs reported in Table 4, a value of 1500 rpm has been chosen. At the end of each run the catalyst was discharged from the reactor and visually inspected to control if particles breakup has occurred. In all cases, also at the higher stirrer speed, no appreciable formation of smaller pieces of resin was observed, so, in principle, the catalyst is reusable. Moreover, it is also important to point out that, in an industrial perspective, the resin is used in a packed bed reactor in which no stirring occurs.

3.2. Internal diffusive phenomena

As a preliminary activity, prior to the kinetic investigation, the influence of the catalyst internal diffusion has been evaluated by

Table 4
Operative conditions of experimental runs in batch reactor.

RUN	Catalyst (g)	Substrate	T (°C)	Initial pressure (bar g)	Amount of catalyst (g)	Amount of soybean oil (g)	Amount of OA or oleins (g)	Initial acidity[a] %	Amount of methanol (g)	MeOH/acid (mol/mol)
1	Uncatalyzed	OA-soy[b]	100	4.3	–	101.8	98.2	49.1	89.1	8:1
2		OA-soy	120	5.1	–	99.6	100.4	50.2	91.1	8:1
3		Oleins	100	4.5	–	–	130.0	92.4	88.1	6.5:1
4		Oleins	120	5.5	–	–	130.0	92.3	88.4	6.5:1
5	Amberlyst	OA-soy	80	2.8	5.08	99.2	100.8	50.4	91.2	8:1
6	15	OA-soy	90	3.9	5.01	100.8	99.2	49.6	90.0	8:1
7		OA-soy	100	4.5	1.00	103.8	96.2	48.1	87.3	8:1
8		OA-soy	100	4.3	3.10	101.4	98.6	49.3	89.5	8:1
9		OA-soy	100	4.4	5.01	100.2	99.8	49.9	90.5	8:1
10		OA-soy	100	4.5	10.00	95.6	104.4	52.2	94.7	8:1
11		OA-soy	120	5.0	5.00	106.0	94.0	47.0	85.3	8:1
12[c]		OA-soy	120	5.3	5.00	102.4	97.6	48.8	88.5	8:1
13	Relite	OA-soy	100	4.3	5.00	102.0	98.0	49.0	88.9	8:1
14	CFS	Oleins	100	4.2	3.06	–	130.0	92.9	87.1	6.5:1
15		Oleins	100	4.3	5.01	–	130.0	92.9	87.1	6.5:1
16		Oleins	120	5.1	3.00	–	130.0	92.9	87.1	6.5:1
17[c]		Oleins	120	5.2	3.01	–	120	92.9	87.1	6.5:1
18	Amberlyst 16	OA-soy	100	4.0	5.04	97.2	102.8	51.4	92.5	8:1
19	Amberlyst 131	OA-soy	100	4.3	5.03	95.2	104.8	52.4	95.0	8:1

[a] Expressed as % of oleic acid.
[b] Mixture oleic acid–soybean oil.
[c] Powdered catalyst.

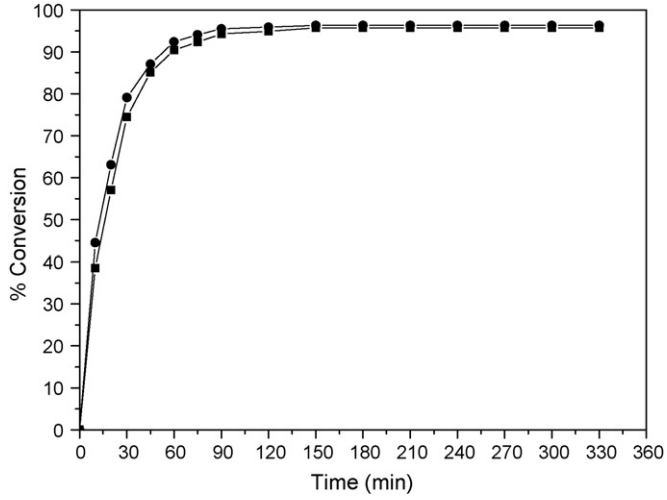

Fig. 3. Comparison of Amberlyst 15 in spheres and powdered. Operative conditions: 5 g of catalyst, temperature 120 °C, substrate oleic acid–soybean oil, molar ratio methanol/acid 8:1. (■) Catalyst spheres (run 11) and (●) catalyst powder (run 12).

means of a test performed on powdered catalyst compared with catalyst in its usual form of spheres. In Figs. 3 and 4 such results are reported for both Amberlyst 15 (T = 120°, 5 g of catalyst, substrate: model mixture oleic acid/soybean oil) and on Relite CFS (T = 120°, 5 g of catalyst, substrate: oleins). For each catalyst the results are related to both powder and spheres and, as it can be observed, the conversion-time profiles are quite similar for both Amberlyst 15 (Fig. 3, runs 11 and 12) and Relite CFS (Fig. 4, runs 16 and 17). This behavior seems to indicate that the catalyst effectiveness factor is close to unity and allows to neglect the limitations on the reaction due to the internal mass transfer resistance.

3.3. Catalytic screening

A first set of experimental runs has been conducted with the scope of comparing the catalytic activity of different ionic exchange resins such as: Amberlyst 15 (run 9), Amberlyst 16 (run 18), Amberlyst 131 (run 19) and Relite CFS (run 13). These runs have been performed at a fixed temperature of 100 °C, with 5 g of catalyst and on an artificially acidified soybean oil with oleic acid. In Fig. 5 the conversion of oleic acid is reported as a function of

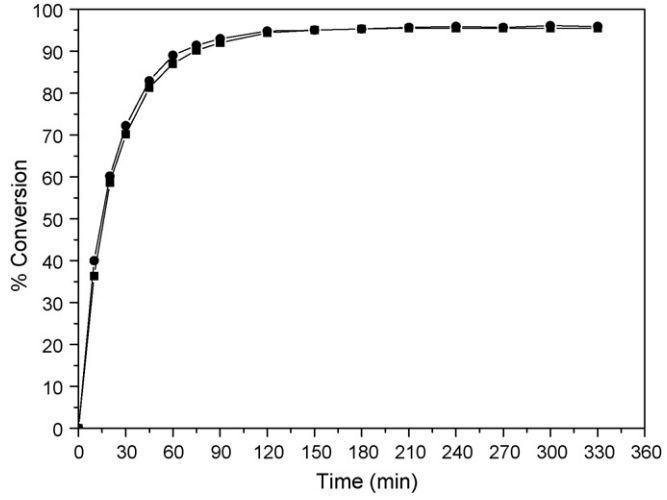

Fig. 4. Comparison of Relite CFS in spheres and powdered. Operative conditions: 3 g of catalyst, temperature 120 °C, substrate oleins, molar ratio methanol/acid 6.5:1. (■) Catalyst spheres (run 16) and (●) catalyst powder (run 17).

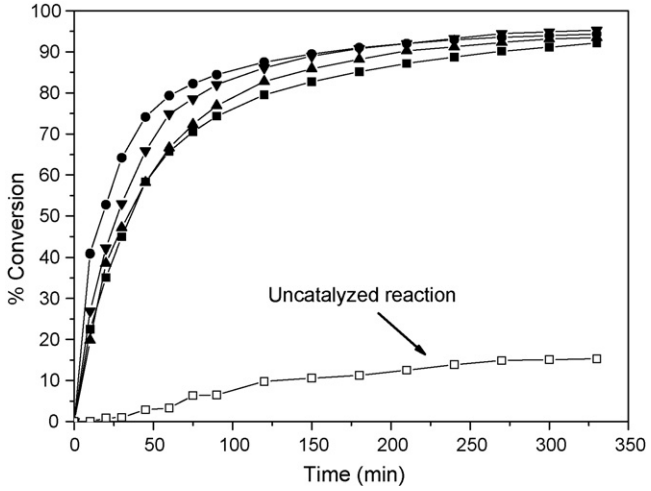

Fig. 5. Experimental batch run for catalytic screening. Operative conditions: 200 g of oleic acid/soybean oil at 50% of acidity; methanol:oleic acid molar ratio = 8:1; weight of catalyst = 5 g; temperature = 100 °C; rpm = 1500. (■) Amberlyst 15—run 9, (●) Amberlyst 16—run 18, (▲) Amberlyst 131 and (▼) Relite CFS. The behavior of uncatalyzed reaction is also reported for comparison (□).

reaction time for, respectively, the runs 9, 13, 18 and 19. From this plot, a comparable activity can be observed for catalysts Amberlyst 15 and Amberlyst 131, while, quite better resulted the performances related to Amberlyst 16 and Relite CFS. On the basis of these obtained preliminary screening results, a more detailed study has been performed on both Amberlyst 15 (more studied in the literature) and on Relite CFS (apparently more active and less expensive).

3.4. Development of the kinetic model

3.4.1. Uncatalyzed esterification

First of all, a preliminary study has been performed on the reaction in the absence of the resin catalyst with the scope of evaluating the contribution of the uncatalyzed reaction on the overall kinetics. Batch runs 1–4 have been made on both the two different previously mentioned substrates in the temperature range of 100–120 °C. The runs performed are described in Table 4. The collected experimental data, related to the uncatalyzed reaction, have been correlated with a pseudo-homogeneous model by considering the reacting mixture as a single liquid phase and neglecting both the liquid–liquid eventual separation and the amount of volatiles compounds (mainly methanol and water) that are present in the head space of the reactor. This assumption was justified by an approximate estimation that, in correspondence of about 2.8 moles of methanol loaded in the reactor, only 0.048 moles (ideal gas approximation) are present in the vapor space that is a negligible quantity. This consideration made for methanol is mostly valid for water that is less volatile. The kinetic expression for the reaction rate is the following:

$$r_{uc} = kC_A^2 C_M - k_{-1} C_A C_W C_E \simeq kC_A^2 C_M \quad (2)$$

where r_{uc} is the reaction rate for the uncatalyzed reaction, C_A and C_M are the liquid phase bulk concentrations of, respectively, oleic acid or other mixtures of fatty acids and methanol, k is the forward kinetic constant, k_{-1} is the reverse kinetic constant. The second order with respect to the acid reactant is suggested by different authors [6,13,17,20], because, this compound would act both as catalyst (in homogeneous phase) and reactant. In derivation of the expression (2) we have also neglected the reverse term of the equilibrium reaction because the reactive system is always far from equilibrium conditions.

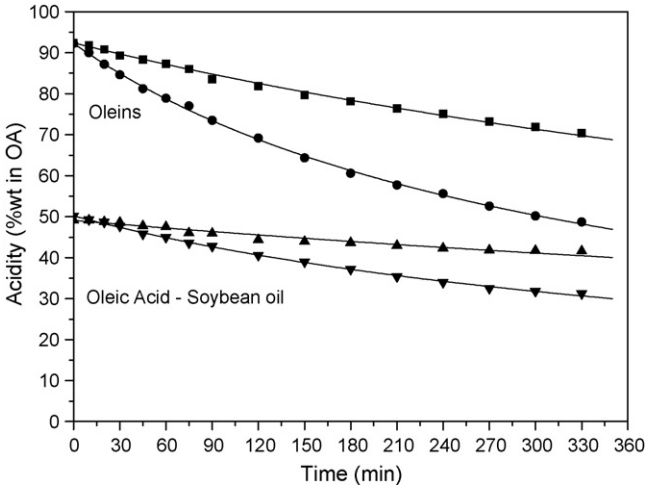

Fig. 6. Experimental batch run for uncatalyzed reaction. (▲) Oleic acid–soybean oil at 100 °C (run 1). (▼) Oleic acid–soybean oil at 120 °C (run 2). (■) Oleins at 100 °C (run 3). (●) Oleins at 120 °C (run 4). (—) Simulated acidity.

According to a modified Arrhenius equation, the reaction rate can be expressed as a function of temperature in the following way:

$$k = k^{\mathrm{ref}} \exp\left[\frac{E_A}{R}\left(\frac{1}{T^{\mathrm{ref}}} - \frac{1}{T}\right)\right] \quad (3)$$

In the expression (3) k^{ref} is the kinetic constant at a reference temperature T^{ref} chosen at 373.16 K while R is the universal gas constant.

The mass balance for the isothermal batch reactor is then defined through the following system of ordinary differential equation (ODE), one for each component in the reacting system, to be solved starting from initial values of the concentrations:

$$\frac{dn_i}{dt} = \nu_i r_{\mathrm{uc}} V_L, \quad \text{with } i = \mathrm{A(Oleic\ acid\ or\ olein)},\ \mathrm{M(methanol)},\ \mathrm{E(methyl\ ester)},\ \mathrm{W(water)} \quad (4)$$

where n_i is the number of moles of the component i, ν_i is the corresponding stoichiometric coefficient i, V_L is the reaction volume evaluated with the ideal hypothesis of volumes additivity and using the densities of each component at the reaction temperature.

The kinetic parameters in the expressions (2)–(4) have been evaluated by nonlinear fitting minimizing the following objective function represented by a quadratic mean square error between the experimental and calculated acidities.

$$\mathrm{RMS} = \sqrt{\frac{1}{N}\sum_{i=1}^{N}(a_i^{\mathrm{exp}} - a_i^{\mathrm{calc}})^2} \quad (5)$$

Fourth order Runge–Kutta method was used to integrate the ODE system (4) at each iteration of the minimization algorithm used in nonlinear least squares fitting.

In Fig. 6, the regression curve for experimental runs 1–4 are reported, while in Table 5, the values of kinetic parameters for the uncatalyzed esterification reaction are reported. An activation energy of about 16 kcal mol^{-1} has been found, in agreement with the values, for similar reactive systems, respectively obtained by Popken et al. [17] for acetic acid esterification and by Sanz et al. [13] for lactic acid esterification.

Table 5
Kinetic parameters of the uncatalyzed esterification (runs 1–4).

Parameter	Oleic acid–soybean oil	Oleins
k^{ref} (ref = 343.16 K) (cm^6 mol^{-2} min^{-1})	88.98	65.78
Activation energy E_A (kcal mol^{-1})	16.48	16.28
Pre-exponential factor A (cm^6 mol^{-2} min^{-1})	4.06×10^{11}	2.29×10^{11}
RMS error	0.854	0.930

3.4.2. Catalyzed esterification

In a previous work, Tesser et al. [20] proposed some kinetic models (pseudo-homogeneous and Eley–Rideal type) for describing the esterification reaction catalyzed by Amberlyst 15 but these models neglect the physico-chemical phenomenology that is the basis of the use of ionic exchange resins as catalysts: the phases partition phenomenon and the ionic exchange equilibrium. The consequence of this simplification involves that the model cannot accurately describe the runs performed in the presence of different catalysts concentrations, particularly in conditions near to the equilibrium. This is because a great amount of catalyst retains selectively more water altering the equilibrium conditions. This has a dramatic effect in tubular packed bed reactors in which the ratio between catalyst and fluid phase reacting mixture is normally much higher.

3.4.2.1. Partition model. The description of the partitioning phenomenon, due to the high swelling ratio of the polymeric resins, is of particular relevance when acid ionic exchange resins are used as catalyst in esterification reactions in which water is always formed as a reaction product and, as mentioned, is more selectively retained by the resin with respect to methanol. First of all, a swelling effect is observed. The swelling phenomenon depends on several factors like: (i) the nature of the solvent (polar, apolar); (ii) the degree of polymer cross-linking; (iii) the nature of the fixed ionic groups; (iv) the exchange capacity; (v) the form and size of solvation shell. According to Helferrich [21] a rigorous and general theory for equilibria with ion-exchangers does not yet exist and would be very complex. For this reason, and according to the purpose of this work, we have developed a simplified model for the description of both the swelling as consequence of the solvation and the partitioning phenomenon. Our proposed model starts with the observation that the driving force for the absorption of a pure component is the difference in the osmotic pressure between the external and internal part of the resin [21]. There is first of all a tendency of the fixed and mobile ions to form stable solvation shells with some molecules of the solvent. Then, the highly concentrated solution of ions inside the exchange resin has a tendency to dilute itself by absorbing additional solvent [21]. A third expanding force is related to the electrostatic interactions and all this expanding forces decrease as swelling progresses [21]. Inside the particles there are fixed anionic groups ($-SO_3^-$), bonded to the surface of the polymer, and relatively mobile protonated molecules like methanol or water. Each charged group, fixed or mobile, can then form a primary solvation shell containing 4–6 molecules as in the following simplified scheme:

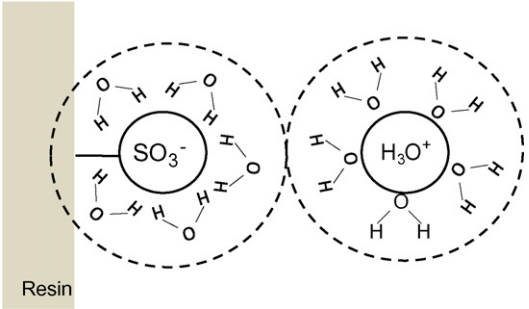

Obviously, other molecules can enter and aggregate to form greater clusters as a consequence of the solvation effect giving place to swelling of the resin. The phenomenon is contrasted by the cross-links of the polymeric matrix in correspondence to the maximum

increasing volume. Pure methanol and water give place to a different swelling ratio. Moreover, the addition of water to a polymer saturated with methanol gives place to a cluster of mixed composition as described by Fujii et al. [22]. We have studied in detail the influence of water/methanol composition on the swelling and the results will be published in a future devoted paper. Besides, on the basis of this study we can conclude that: (i) swelling is poorly affected by the temperature, (ii) oil phase gives no place to swelling, (iii) in the presence of an excess of methanol, the presence of water poorly affects the swelling ratio and, consequently, the absorbed volume. We have tested the effect of water on the absorbed liquid volume in the range 0–50 wt% of water for both the resins A-15 and R-CFS. In this range of water concentration the swelling ratio resulted poorly affected and vary from 1.52 to 1.59 for A-15 and from 1.71 to 1.80 for R-CFS. Therefore, the internal volume accessible to the reaction mixture is about the same determined in the presence of pure methanol corresponding to about 0.609 and 0.790 (mL g_{res}^{-1}) for, respectively Amberlyst 15 and Relite CFS (the corresponding swelling ratio are 1.519 and 1.714, respectively). Knowing the resin accessible volume, in order to evaluate the partition of the binary mixture methanol–water, we suggest to consider that each molecule (for example of methanol) inside the particle, occupies a definite site in the available space volume characterized by a particular energy level according to its position (primary shell or surroundings). Water molecules, formed by the esterification reaction or coming from the external liquid bulk, displace methanol molecules instauring the partition equilibrium. Considering that the mentioned sites are distributed in the internal volume and that the available volume is fixed, a volume based Langmuir expression can easily be derived considering as driving force the volume filling degree with an approach very similar to the classical Langmuir based on surface coverage degree. Therefore, we can write for the forward (absorption) and reverse (desorption) reaction rates:

$$r_i^{abs} = k_i^{abs} C_i^B \phi_f^R V^{abs} \quad (6)$$

$$r_i^{des} = k_i^{des} \phi_i^R V^{abs} \quad (7)$$

In the relations (6) and (7) k_i^{abs} and k_i^{des} are the kinetic constants for, respectively the absorption and desorption processes, ϕ_i^R is the volumetric fraction of the ith component inside the resin particles and ϕ_f^R is the fraction of volume in which the absorption is allowable. In equilibrium conditions, relations (6) and (7) can be equated and a definition of the absorption constant K_i can be straightforwardly derived:

$$K_i = \frac{k_i^{abs}}{k_i^{des}} = \frac{\phi_i^R}{C_i^B \phi_f^R} \quad (8)$$

For the complete definition of the model, a further equation is necessary, that is the relation between the volumetric fraction and the internal concentration of the resin:

$$\phi_i^R = \frac{C_i^R M w_i}{\rho_i} \quad (9)$$

The value of V^{abs}, appearing in Eqs. (6) and (7), can be calculated through the following relation:

$$V^{abs} = \frac{(S-1)(1-\varepsilon)}{\rho_{bulk}^{dry}} \quad (10)$$

where S is the swelling ratio and ρ_{bulk}^{dry} represents the bulk density of dry resin and ε the void fraction external to the particles that has been assumed, for relatively uniform spheres, equal to about 0.35 [23].

According to the proposed partitioning model, for a multicomponent mixture, the following Eq. (11) can be used for relating the external (superscript B) to the internal (superscript R) concentration for each of the partitioned components:

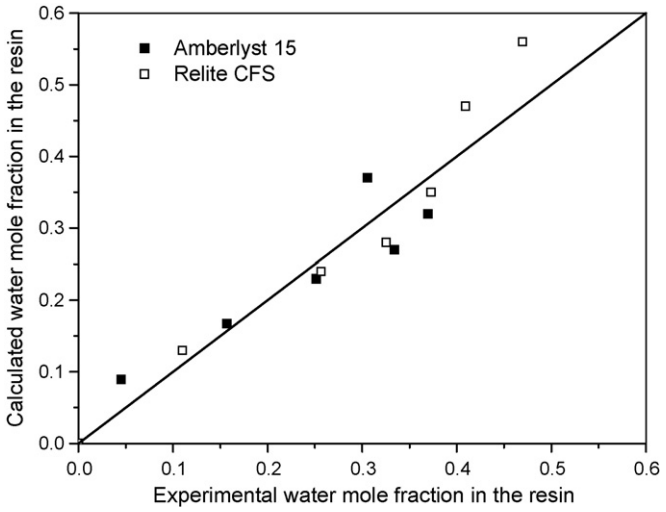

Fig. 7. Parity plot. Calculated vs experimental water mole fraction in the resin.

$$C_i^R = \frac{K_i^{eff} C_i^B}{\sum_j K_j C_j^B} \quad (11)$$

where C_i^R and C_i^B are the concentrations of the ith component in the bulk phase and inside the resin, respectively, K_j is the partition constant, while, K_i^{eff} represents the effective partition constant that takes into account for the molecular size of the pure ith component through the introduction of its molar density ρ_i and molecular weight M_i through the relation (12).

$$K_i^{eff} = \frac{K_i \rho_i}{M_i} \quad (12)$$

In the relation (12) the partition constants K_i are determined from experimental absorption data of the corresponding binary system as explained below.

In our specific system, the physical equilibrium for triglycerides partition has been neglected due to their relatively high molecular size. The partition parameters related to the binary system water/methanol have been determined on the basis of the experimental data of Table 3. The reliability of the proposed partition model can be appreciated in Fig. 7 where the parity plot, for partitioning runs performed at 100 °C for both the resins Amberlyst 15 and Relite CFS, is reported.

All the parameters related to the partitioning model used in the present work, are reported in Table 6 and have been evaluated, for both the resins Amberlyst 15 and Relite CFS, at 100 °C. This temperature was assumed as an average temperature value and the corresponding data have been considered valid also in the range of 90–120 °C in which the experimental esterification runs have been conducted.

Table 6
Parameters for the partition model.

Component	Amberlyst 15		Relite CFS	
	K_i (mL mol^{-1})	K_i^{eff}	K_i (mL mol^{-1})	K_i^{eff}
Water	1	0.0542	1	0.0542
Methanol	0.519	0.0113	0.317	0.0069
Fatty acid[a]	1	0.0029	1	0.0030
Methyl ester	0.519	0.0014	0.317	0.00088

[a] Oleic acid in the case of Amberlyst 15 and oleins for Relite CFS.

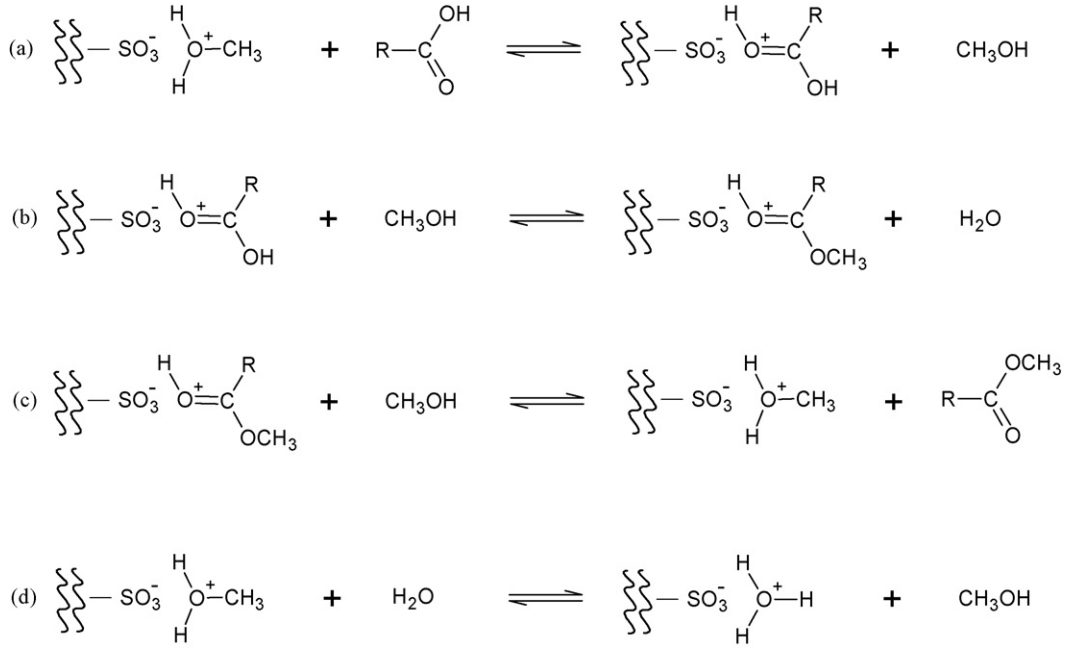

Fig. 8. Scheme of reaction mechanism for the esterification catalyzed by ion-exchange acid resins.

The same parameters, related to the other binaries, in the absence of experimental data, have approximately estimated on the basis of the following considerations. For what concerns the fatty acids and their corresponding methylesters, we have assumed that the differences in polarity and molecular sizes among them are almost the same of those between water and methanol. In such a way, as a rough approximation, the partition constant for the fatty acid is assumed equal to that of water ($K_A = K_W$), while the constant for methylester is assumed equal to that of methanol ($K_E = K_M$). With this assumptions, the effective partition constants determine the competitive adsorption of the various components in the quaternary system considered (methanol, water, methylester and fatty acid) according to their molecular weight (molecular size) and polarity.

3.4.2.2. Reaction mechanism. When acid ionic exchange resins are used as catalysts, the active site is the sulphonic group that exchange the hydrogen ion with the components involved in the reaction adsorbed on the resin surface. The reactants are then subjected to a physical absorption equilibrium and to a successive protonic exchange equilibrium reaction. The proposed kinetic model keeps into account for both these aspects and is based on the following hypotheses: (i) all the active sites of the resin are occupied and, in particular, the major part of them is occupied by the methanol in a protonated form. This hypothesis is justified by the high methanol molar excess used in the experimental runs (molar ratio methanol/oleic acid > 6.5:1) with respect to the other components and by considering that, initially, water is not present in the reacting medium. So methanol will be preferably adsorbed with respect to fatty acid; (ii) all the components (fatty acid, water and methylester) undergo to a protonic exchange equilibrium with the protonated methanol adsorbed onto the active sites; (iii) the reactive event occurs through an Eley–Rideal mechanism between a protonated fatty acid and the methanol coming from the liquid phase absorbed inside the resin particles. The scheme of exchange and reaction steps is reported in Fig. 8.

The step (a) represents the exchange between fatty acid and protonated methanol; the step (b) is the Eley–Rideal surface reaction that involves the protonated fatty acid and methanol. This reaction leads to the formation of protonated methylester and the corresponding amount of water that is partitioned between the internal (absorbed) liquid phase and the external (bulk) liquid phase. The water present in the internal liquid phase can then be involved in an exchange equilibrium with protonated methanol giving place to a competition on the active site, as expressed by step (d). Finally, the step (c) represents the exchange reaction between the protonated methylester and methanol from the internal liquid phase that, contemporarily, restore the active size with protonated methanol and release the methylester that is partitioned between the internal and the external liquid phase.

By assuming that the Eley–Rideal reactive event (step (b) in Fig. 8) is the rate determining step (RDS) for the overall kinetics, the following expression (13) can be derived for the reaction rate:

$$r_{cat} = \frac{k_{cat} H_A C_A^R - k_{-cat} \frac{H_E C_E^R C_W^R}{C_M^R}}{1 + \frac{H_A C_A^R}{C_M^R} + \frac{H_E C_E^R}{C_M^R} + \frac{H_W C_W^R}{C_M^R}} \quad (13)$$

In relation (13) k_{cat} and k_{-cat} are the kinetic constants for, respectively, the forward and the reverse catalyzed reaction that are both functions of temperature according to Arrhenius relation (Eq. (3)); H_A, H_W and H_E are the ionic exchange equilibrium constants for the reactions of protonated methanol with, respectively, fatty acid, water and methylester; C_i^R is the concentration of the various components in the resin-absorbed liquid phase. In the narrow explored temperature range, we have assumed that the constants H_A, H_W and H_E are independent from temperature.

3.5. Reactor model

In the development of a suitable reactor model, we have made the assumption that the system is always in physical equilibrium in a way that the internal concentration of the reactants and products can be evaluated from the corresponding bulk concentrations according to Eq. (11). The evolution with time of the moles of each component can be evaluated by solving the following material balance based on a set of ordinary differential equation (ODE)

expressed by the relation (14):

$$\frac{dn_i}{dt} = \nu(r_{uc}V_L + r_{cat}W_{cat}) \quad (14)$$

where n_i represents the overall mole number of the ith species and W_{cat} is the weight of catalyst loaded in the reactor. At each integration step in time of the system (14) the partitioning equilibrium must be solved by imposing the congruence balance Eq. (15):

$$n_i^R + n_i^B = n_i \quad (15)$$

where n_i^R and n_i^B are, respectively, the moles of ith component in the resin and in the bulk. The number of moles n_i^R is obtained as simultaneous solution of the set of nonlinear algebraic equations (11) and the explicit algebraic equation (16):

$$n_i^R = C_i^R V^{abs} W_{cat} \quad (16)$$

where V^{abs} is the volume of adsorbed liquid phase per gram of catalyst.

By considering the used high excess of methanol, the quantity of water formed during the reaction is less than 10% in weight with respect to the charged methanol. In these conditions it is reasonable to assume that V^{abs} is equal to the specific volume adsorbed in the case of pure methanol (0.609 cm^3/g_{res} for Amberlyst 15 and 0.790 cm^3/g_{res} for Relite CFS [20]). In other words, in the application of our model for reactor simulation, we have neglected the variation of the specific adsorbed volume with the liquid phase composition.

The moles in the bulk phase, n_i^B, are calculated from Eq. (15) while the bulk concentration is evaluated from the following relation (17):

$$C_i^B = \frac{n_i^B}{V_L}. \quad (17)$$

3.6. Description of the experimental batch runs

The experimental runs reported in Table 4, devoted to the kinetic analysis of the resin-catalyzed reaction (runs 5–11 for Amberlyst 15 and runs 13–16 for Relite CFS), have been interpreted by means of a commercial ODE solver (Berkeley Madonna®) in which the 7 adjustable parameters of the model (k_{cat}^{ref}, $E_{A,cat}$, k_{-cat}^{ref}, $E_{A,-cat}$, H_A, H_W, H_E) have been evaluated by minimizing the root mean square error (RMS, Eq. (2)) between the experimental and calculated data. The best-fit parameters are reported in Table 7 for both the examined catalysts. From the values of the ionic exchange constants related to both the resins, we can observe that the only value greater than one is that referred to water. This means that the more stable protonated species is that of water bonded to the acidic site corresponding to a strong water competition with respect to the others components present in the mixture. Moreover, by comparing these constants, we can conclude that the equilibrium exchange water–methanol results favored with respect to the other two equilibria of this kind: fatty acid–methanol and methylester–methanol.

In Fig. 9 the acidity–time profiles for the runs performed with 5 g of Amberlyst 15, on a model mixture oleic acid/soybean oil, at different temperatures (runs 5, 6, 9, 11) are reported. The temperature dependence of the constant for Amberlyst 15 is defined by an activation energy (related to the forward reaction) of 17 kcal/mol, a value in a close agreement to that found by Popken et al. [17] of 16 kcal/mol for the esterification of acetic acid with methanol on the same catalyst.

In Fig. 10, the acidity–time profiles are reported for the runs performed, at 100 °C, with different Amberlyst 15 concentrations (runs 7–10), with the model mixture as in the previous set of runs. We can observe that the dependence on the catalyst concentration of the reaction rate is well described by the model, especially in the final part of the runs. As the chemical equilibrium constant is the same

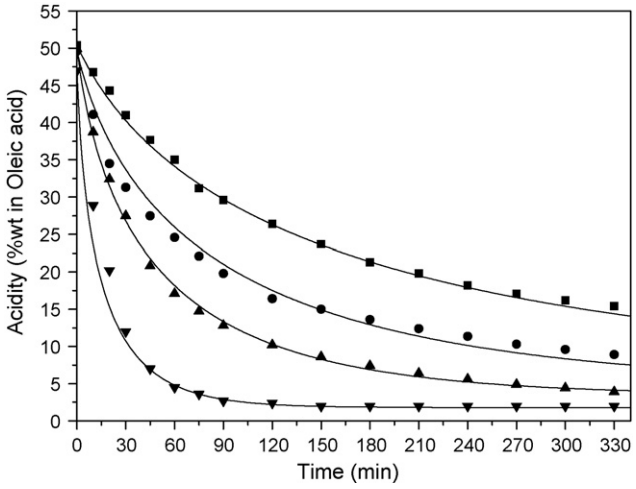

Fig. 9. Experimental batch run for esterification catalyzed by Amberyst 15 at different temperatures. Substrates: oleic acid–soybean oil; catalyst loading: 5 g. (■) 80 °C (run 5), (●) 90 °C (run 6), (▲) 100 °C (run 9) and (▼) 120 °C (run 11). (—) Simulated acidity.

for all the considered runs, the presence of different final plateau shown in Fig. 10 means that in the presence of different amounts of catalyst, the equilibrium reached inside the catalyst particles is different for the different amounts of retained water. This behavior is much more evident when a tubular reactor of pilot or industrial size is employed, because, it is not possible to simulate their behavior by using another model neglecting the effect of the selective partition. These aspects are emphasized in the comparison reported in Fig. 11, where, the final part of the previously mentioned runs are respectively interpreted with a pseudo-homogeneous model neglecting the partition phenomenon and the model proposed in this work. As it can be seen the pseudo-homogeneous model that is able to describe runs performed at different temperatures with the same amount of catalyst, completely fails in describing runs performed at the same temperature but changing the amount of catalyst. On the contrary the partition model gives a good agreement in both cases.

In Fig. 12, the acidity profiles for the runs performed with Relite CFS as catalyst on oleins as substrate, adopting different temperatures and catalysts concentrations, are reported. The dependence

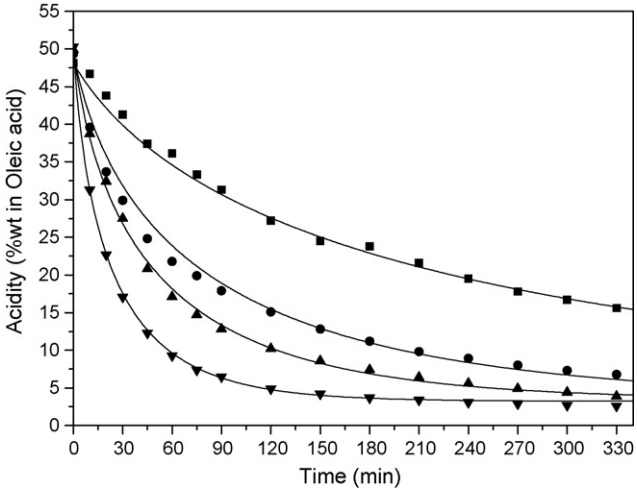

Fig. 10. Experimental batch run for esterification catalyzed by Amberyst 15 at different catalysts loading. Substrates: oleic acid–soybean oil; temperature: 100 °C. (■) 1 g (run 7), (●) 3 g (run 8), (▲) 5 g (run 9) and (▼) 10 g (run 10). (—) Simulated acidity.

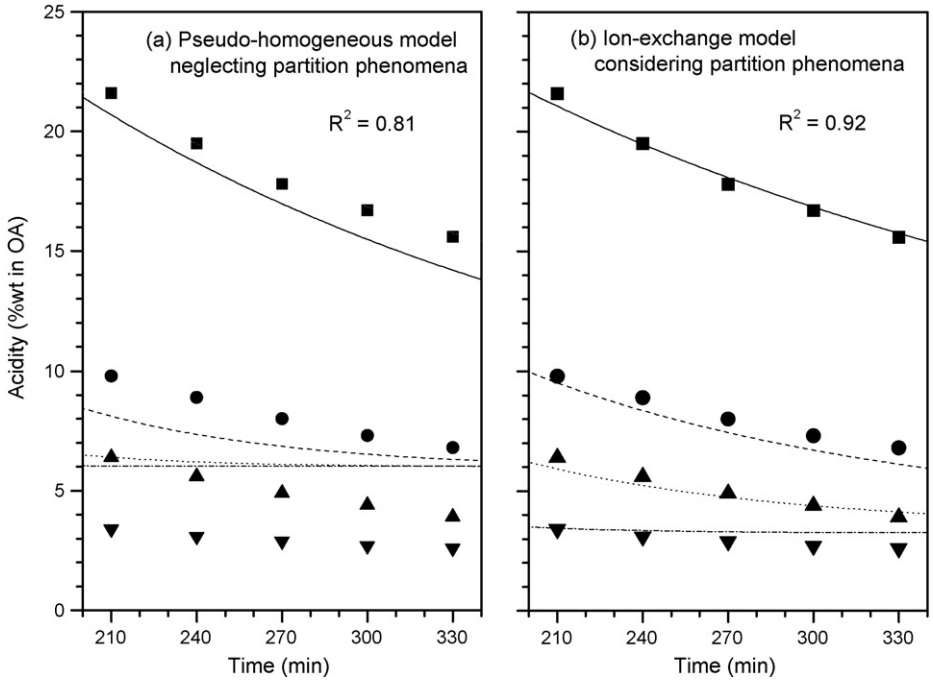

Fig. 11. A comparison between pseudo-homogeneous model and partition model, proposed in this work, in the description of the final part of runs performed at 100 °C in the presence of different amounts of catalyst (Amberlyst 15). (■) 1 g (run 7), (●) 3 g (run 8), (▲) 5 g (run 9) and ▼ 10 g (run 10). (—) Simulated acidity.

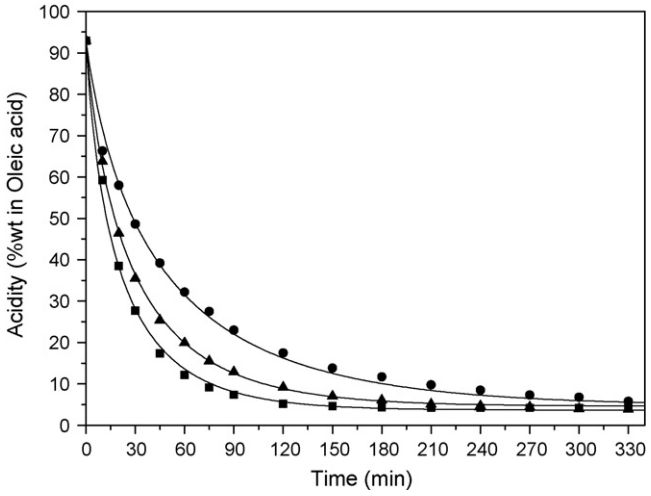

Fig. 12. Experimental batch run for esterification of oleins catalyzed by Relite CFS. (■) 1 g (run 7), (●) 3 g at 100 °C (run 14), (▲) 5 g at 100 °C (run 15) and (▼) 3 g at 120 °C (run 16). (—) Simulated acidity.

of the reaction rate from temperature has been evaluated by means of two runs (runs 14 and 16) at 100 and 120 °C, respectively and an activation energy of 13 kcal/mol has been evaluated for the forward reaction, quite similar to that related to Amberlyst 15. By observing the agreement between the experimental runs 14 and 15 and the model results, also for this catalyst the model is again able to describe the dependency on the catalyst concentration. The kinetic and ionic exchange constants, evaluated as for the previous catalyst, are reported in Table 7 from which we can observe that water–methanol exchange constant for Relite CFS is about 3 times lower than the same parameter for Amberlyst 15.

In conclusions, from Figs. 9, 10 and 12, we can observe that the kinetic and physical equilibrium model, developed in this work, are characterized by an high accuracy degree in the description of the collected experimental data and are also able to correctly interpret the physical phenomena occurring when ion-exchange resins are used as esterification catalysts (swelling and partitioning).

In order to better emphasize the characteristics of the proposed model, in Fig. 13 a simulation result is reported in terms of the amount of water retained by the resin during the reaction. These profiles are referred to the run 10 with Amberlyst 15 (10 g of catalyst) and it is interesting to observe that, at the end of the reaction, about 6 g of water were globally produced and this overall amount is partitioned as follows: about 1 g inside the resin and the remaining 5 g outside. Considering the ratio between the external and the internal volumes, it is evident that the internal concentration of water is much higher than the external one and also than the overall concentration (if the partition of water is neglected). This consideration clearly indicates that the presence of such catalysts strongly affects the concentration and consequently, being the local concentrations very different from the overall ones, the kinetics of the process.

Table 7
Kinetic and ion-exchange parameters.

Resin	Kinetic parameters				Ion-exchange equilibrium constant			RMS
	k_{cat}^{ref} ($cm^3\ gcat^{-1}\ min^{-1}$)	$E_{A,cat}$ ($kcal\ mol^{-1}$)	k_{-cat}^{ref} ($cm^3\ gcat^{-1}\ min^{-1}$)	$E_{A,-cat}$ ($kcal\ mol^{-1}$)	H_A	H_W	H_E	
Amberlyst 15[a]	9.01	17.46	5.50	8.78	0.46	4.74	0.13	7.02
Relite CFS[b]	13.07	12.77	3.85	7.96	0.31	1.55	0.17	3.35

[a] Regression on experimental runs 5–11 reported in Table 3.
[b] Regression on experimental runs 13–16 reported in Table 3.

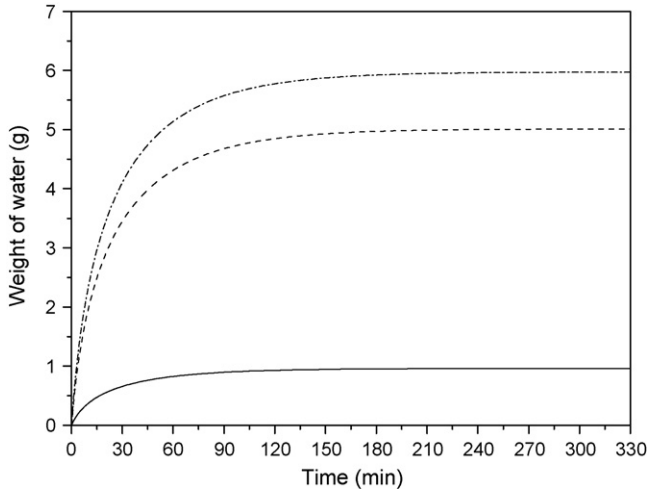

Fig. 13. Simulation of the water partition for the experimental run 10. Catalyst: 10 g of Amberlyst 15; temperature: 100 °C; substrate: oleic acid–soybean oil. (—) Simulated amount of water in the interior of the resin. (– – –) Simulated amount of water in the external bulk phase. (– · –) Simulated total amount of water.

4. Conclusions

In this paper the esterification reaction of free fatty acids in high-acidity substrates has been studied and modeled. Different acid ionic exchange polymeric resins have been tested as catalysts in a batch reactor and two of them have been selected after a preliminary screening. On the selected catalyst (Amberlyst 15 and Relite CFS) different kinetic runs have been performed and the influence of temperature and catalyst concentration has been studied. A detailed kinetic/equilibrium model has been developed, for the description of the collected experimental data, taking into account for the following aspects: (i) the physical phase equilibrium (partitioning equilibrium) of the components between the liquid absorbed phase inside the resin and the external liquid phase also considering the swelling effect of the resin on the internal volume; (ii) the ionic exchange equilibria between protonated methanol and other molecules; (iii) a Eley–Rideal surface reaction mechanism in which a protonated fatty acid reacts with methanol coming from the liquid phase absorbed by the particles. The model allows a good description of the kinetic behavior, also in the region close to the chemical equilibrium, in particular for runs performed at different catalyst concentrations. Such result makes the model suitable, in perspective, for an accurate simulation of the behavior of continuous pilot or industrial tubular reactors.

Acknowledgement

Thanks are due to the Italian Ministry of Foreign Affairs (MAE) for the financial support.

List of symbols

a	acidity (%wt in oleic acid)
C	concentration (mol mL^{-1})
C_{titr}	concentration of titrant (mol mL^{-1})
E_A	activation energy (kcal mol^{-1})
H	ionic exchange equilibrium constant
k	kinetic constant of uncatalyzed reaction (mL^2 mol^{-2} min^{-1})
k_{cat}, k_{-cat}	kinetic constants of the forward and the reverse reaction (mL^{-1} g_{cat}^{-1} min^{-1})
k^{abs}	kinetic constant for absorption process (min^{-1})
k^{des}	kinetic constant for desorption process (mol min^{-1} cm^{-3})
K	partition constant (mL mol^{-1})
K^{eff}	effective partition constant
M	molecular weight (g mol^{-1})
m_{sample}	weight of sample (g)
N	number of experimental data
n	number of moles (mol)
R	universal gas constant (kcal mol^{-1} K^{-1})
r_{cat}	rate of catalyzed reaction (mol min^{-1} g_{cat}^{-1})
r_{uc}	rate of uncatalyzed reaction (mol min^{-1} cm^{-3})
r	rate for absorption and desorption process (mol min^{-1} g^{-1}_{res})
RMS	root mean square error
S	Swelling ratio
T	Temperature (K)
t	time (min)
V_L	liquid volume (mL)
V^{abs}	volume of adsorbed liquid phase per gram of catalyst (mL g_{cat}^{-1})
V_{titr}	volume of titrating solution (mL)
W_{cat}	weight of catalyst (g)
ν	stoichiometric coefficient
ρ	molar density (mol cm^{-3})
ε	inter-particles void fraction
ρ^{dry}_{bulk}	bulk density of dry resin (g cm^{-3})
ϕ	volumetric fraction

Subscript

A	oleic acid
E	methyl ester
i	index for ith component
M	methanol
W	water
T	triglycerides

Superscript

B	bulk-external of resin
calc	calculated value
exp	experimental data
R	internal of resin
ref	reference temperature, 373.16 K

References

[1] F. Ma, M.A. Hanna, Biodiesel production: a review, Bioresour. Technol. 70 (1999) 1–15.
[2] H. Fukuda, A. Kondo, H. Noda, Biodiesel fuel production by transesterification of oils, J. Biosci. Bioeng. 92 (2001) 405–416.
[3] J.H. Van Gerpen, Biodiesel Economics. Montana Economics, Biological and Agricultural Engineering. University of Idaho, Moscow, ID, USA, 2007, www.deq.state.mt.us.
[4] D. Kusdiana, S. Saka, Kinetics of transesterification in rapeseed oil to biodiesel fuel as treated in supercritical methanol, Fuel 80 (2001) 693–698.
[5] M. Berrios, J. Siles, M.A. Martìn, A. Martìn, A kinetic study of the esterification of free fatty acids (FFA) in sunflower oil, Fuel 86 (2007) 2383–2388.
[6] C. Lacaze-Dufaure, Z. Mouloungui, Catalysed or uncatalysed esterification reaction of oleic acid with 2-ethyl hexanol, Appl. Catal. A: Gen. 204 (2000) 223–227.
[7] P.J. Flory, Principles of Polymer Chemistry, Cornell University, Ithica, NY, 1953.
[8] S. Pasias, N. Barakos, C. Alexopoulos, N. Papayannakos, Heterogeneously catalyzed esterification of FFAs in vegetable oils, Chem. Eng. Technol. 29 (11) (2006) 1365–1371.
[9] J.M. Marchetti, V.U. Miguel, A.F. Errazu, Heterogeneous esterification of oil with high amount of free fatty acids, Fuel 86 (2007) 906–910.
[10] R. Tesser, M. Di Serio, M. Guida, M. Nastasi, E. Santacesaria, Kinetics of oleic acid esterification with methanol in the presence of triglycerides, Ind. Eng. Chem. Res. 44 (2005) 7978–7982.
[11] E. Santacesaria, R. Tesser, M. Di Serio, M. Guida, D. Gaetano, A. Garcia Agreda, Kinetics and mass transfer of free fatty acids esterification with methanol in a tubular packed bed reactor: a key pretreatment in biodiesel production, Ind. Eng. Chem. Res. 46 (2007) 5113–5121.
[12] E. Santacesaria, R. Tesser, M. Di Serio, M. Guida, D. Gaetano, A. Garcia Agreda, F. Cammarota, Comparison of different reactor configurations for the reduction of free acidity in raw materials for biodiesel production, Ind. Eng. Chem. Res. 46 (2007) 8355–8362.

[13] M.T. Sanz, R. Murga, S. Beltràn, J.L. Cabezas, J. Coca, Autocatalyzed and ion-exchange-resin-catalyzed esterification kinetics of lactic acid with methanol, Ind. Eng. Chem. Res. 41 (2002) 512–517.
[14] S.H. Ali, S.Q. Merchant, Kinetics of the esterification of acetic acid with 2-propanol: impact of different acidic cation exchange resins on reaction mechanism, doi:10.1002/kin.20193, published online (www.interscience.wiley.com).
[15] T. Yalcinyuva, H. Deligoz, I. Boz, M.A. Gurkaynak, Kinetics and mechanism of myristic acid and isopropyl alcohol esterification reaction with homogeneous and heterogeneous catalyst, doi:10.1002/kin.20293, published online (www.interscience.wiley.com).
[16] M. Mazzotti, B. Neri, D. Gelosa, A. Kruglov, M. Morbidelli, Kinetics of liquid-phase esterification catalyzed by acidic resins, Ind. Eng. Chem. Res. 36 (1997) 3–10.
[17] T. Popken, L. Gotze, J. Gmehling, Reaction kinetics and chemical equilibrium of homogeneously and heterogeneously catalyzed acetic acid esterification with methanol and methyl acetate hydrolysis, Ind. Eng. Chem. Res. 39 (2000) 2601–2611.
[18] W. Song, G. Venimadhavan, J.M. Manning, M.F. Malone, M.F. Doherty, Measurement of residue curve maps and heterogeneous kinetics in methyl acetate synthesis, Ind. Eng. Chem. Res. 37 (1998) 1917–1928.
[19] S.D. Alexandratos, Ion exchange resins: a retrospective from industrial and engineering chemistry research, Ind. Eng. Chem. Res. 48 (2009) 388–398.
[20] R. Tesser, L. Casale, D. Verde, M. Di Serio, E. Santacesaria, Kinetics of free fatty acids esterification: batch and loop reactor modeling, Chem. Eng. J. (2009).
[21] F.G. Helferrich, Ion Exchange, Dover Science Books, 1995 (Chapter 5).
[22] A. Fujii, S. Enomoto, M. Miyazaki, N. Mikami, Morphology of protonated methanol clusters: an infrared spectroscopic study of hydrogen bond networks of $H^+(CH_3OH)n$ (n = 4–15), J. Phys. Chem. A 109 (1) (2005) 138–141.
[23] T. Kudra, C. Strumillo (Eds.), Thermal Processing of Biomaterials in Topics in Chimica Engineering, vol. 10, Gordon and Breach Science Publisher, 1998, pp. 61–62.